Published in final edited form as:
Circ Cardiovasc Imaging. 2014 January 1; 7(1): 164–172. doi:10.1161/CIRCIMAGING.113.000722.

Validation of Noninvasive Indices Of Global Systolic Function in Patients with Normal and Abnormal Loading Conditions: A Simultaneous Echocardiography Pressure-Volume Catheterization Study

Raquel Yotti, MD, PhD[1], **Javier Bermejo, MD, PhD**[1], **Yolanda Benito, DCS, DVM**[1], **Ricardo Sanz, MD**[1], **Cristina Ripoll, MD, PhD**[2], **Pablo Martínez-Legazpi, PhD**[3], **Candela Péerez del Villar, MD**[1], **Jaime Elízaga, MD, PhD**[1], **Ana González-Mansilla, MD, PhD**[1], **Alicia Barrio, DCS, MBiol**[1], **Rafael Bañares, MD, PhD**[2], and **Francisco Fernández-Avilés, MD, PhD**[1]

[1]Department of Cardiology, Hospital General Universitario Gregorio Marañón and Instituto de Investigación Sanitaria Gregorio Marañón, Madrid, Spain

[2]Department of Gastroenterology and CIBERHD, Hospital General Universitario Gregorio Marañón and Instituto de Investigación Sanitaria Gregorio Marañón, Madrid, Spain

[3]Mechanical and Aerospace Engineering Department. University of California San Diego, La Jolla, CA

Abstract

Background—Noninvasive indices based on Doppler-echocardiography are increasingly used in clinical cardiovascular research to evaluate LV global systolic chamber function. Our objectives were 1) to clinically validate ultrasound-based methods of global systolic chamber function to account for differences between patients in conditions of abnormal load, and 2) to assess their sensitivity to load confounders.

Methods and Results—Twenty-seven patients (8 dilated cardiomyopathy, 10 normal ejection fraction [EF], and 9 end-stage liver disease) underwent simultaneous echocardiography and left heart catheterization with pressure-conductance instrumentation. The reference index, maximal elastance (E_{max}) was calculated from pressure-volume loop data obtained during acute inferior vena cava occlusion. A wide range of values was observed for LV systolic chamber function (E_{max}: 2.8 ± 1.0 mmHg/ml), preload, and afterload. Amongst the noninvasive indices tested, the peak ejection intraventricular pressure difference (peak-EIVPD) showed the best correlation with E_{max} (R=0.75). A significant but weaker correlation with E_{max} was observed for EF (R=0.41), mid-wall fractional shortening (R=0.51), global circumferential strain(R=−0.53), and strain-rate (R=−0.46). Longitudinal strain and strain-rate failed to correlate with E_{max}, as did noninvasive single-beat estimations of this index. Principal component and multiple regression analyses demonstrated that peak-EIVPD was less sensitive to load, whereas EF and longitudinal strain and strain-rate were heavily influenced by afterload.

Correspondence to: Javier Bermejo, MD, PhD, Department of Cardiology, Hospital General Universitario Gregorio Marañón, Dr. Esquerdo 46. 28007 Madrid. SPAIN. javbermejo@jet.es, Telephone: 34-91-5868279, Fax: 34-91-5866727.

Partially presented at the American Heart Association Scientific Sessions, Chicago, IL, November 13th–17th 2010, and published in Abstract form (Circulation 2010; 122: A17816)

Disclosures
None.

Conclusions—Current ultrasound methods have limited accuracy to characterize global LV systolic chamber function in a given patient. The Doppler-derived peak-EIVPD should be preferred for this purpose because it best correlates with the reference index and is more robust in conditions of abnormal load.

Keywords

echocardiography; hemodynamics; systolic function; pressure-volume relationship; imaging

In clinical practice, global left ventricular (LV) systolic function is typically assessed by means of LV volumes and ejection fraction (EF), most frequently measured using echocardiography. However, in metabolic diseases,[1] known[2] or suspected cardiomyopathies,[3] or cardiotoxicity,[4] the evaluation of global systolic chamber function sometimes entails more sensitive and robust indices than EF. In epidemiological research, alternative noninvasive methods derived from Doppler-echocardiography have also proved to be more sensitive than EF to detect subtle abnormalities of systolic function.[5–7] Consequently, several indices have been implemented based on the analysis of myocardial deformation (e.g. global systolic myocardial strain or strain rate),[8] of chamber fluid-dynamics (e.g. intraventricular pressure gradients),[9] and on single-beat approximations to the end-systolic pressure-volume relationship (ESPVR).[10, 11] However importantly, whether these methods account for true global chamber systolic function in the clinical setting has not been clearly established. Also their performance in disease conditions associated to an abnormal systolic load has not been specifically studied.

Invasive indices based on the pressure-volume relationship are the most reliable reference standards to evaluate global LV systolic chamber function in the intact heart.[12] Therefore, the pressure-volume loop method has been used to validate most Doppler-echocardiographic indices of systolic function in animal experiments. However, most of these validation studies have relied on repeated measures experiments in a small number of animals, focusing on acute load and inotropic interventions, frequently in normal ventricles.[8–10, 13] Extrapolating the results of these studies to compare differences in baseline systolic chamber function among patients may be misleading, particularly in the presence of abnormal load confounders.[14]

The objectives of the present study were twofold: 1) to validate Doppler-echocardiographic indices of systolic chamber function against LV maximal elastance (E_{max}) obtained from the ESPVR; and 2) to assess the influence of baseline preload and afterload confounders on noninvasive indices.

Methods

Patients

The study protocol was approved by the local Institutional Review Board, and all subjects provided written informed consent. Twenty-seven patients in sinus rhythm undergoing left heart catheterization were included. Indications for the catheterization procedure were ruling out coronary artery disease in: a) patients with chest pain of unknown etiology with normal EF (n=10), b) patients with dilated cardiomyopathy (n=8), and c)patients with cirrhosis candidates for liver transplantation with more than two cardiovascular risk factors (n=9). Patients with cirrhosis were specifically selected because of their characteristically abnormal preload and afterload.[15] Clinical and demographic data of patients are shown in Table 1. No patient underwent coronary revascularization in the same procedure.

Signal Acquisition Protocol and Pressure-volume Data Analysis

All catheterization procedures were performed by the femoral approach. A high-fidelity pressure-conductance 7F pig-tail catheter (CD-Leycom, The Netherlands) was placed inside the LV, connected to a dual field conductance processor (CD-Leycom CFL-512) and calibrated using the hypertonic saline method.[16] An occlusion balloon (Nu-Vasive 40 mm) was placed at the junction of the inferior vena cava and the right atrium. A Swan-Ganz catheter was used to measure pulmonary pressures, as well as thermodilution cardiac output, and stroke volume (SV). Systemic vascular resistance (SVR) was calculated from invasive recordings of systemic blood pressure. All signals were digitized at 250 Hz. Pressure and volume signals were acquired at end-expiration apnea during transient caval occlusion. To minimize reflex activation, we obtain pressure-volume loops only during de first 5–6 seconds after balloon occlusion. This acquisition process was repeated 3 to 5 times in each patient, waiting for stabilization periods of 5 minutes. E_{max}, defined as the slope of the ESPVR, was calculated using the iterative regression method (Figure 1, Panel A).[16] Effective arterial elastance (E_a) was measured from the pressure-volume loops as the ratio of end-systolic pressure (P_{es}) to SV.[17] End-systolic wall stress () was calculated from the pressure-volume measurements under the assumption of a thick-walled sphere, following:[18, 19]

$$\sigma = P_{es} \cdot \left(1 + 3\frac{ESV}{V_w}\right)$$

The volume of the LV wall (V_w) was obtained as the LV mass divided by myocardial density. In turn, LV mass was measured from 3D-echocardiographic sequences and calibrated (see Supplemental Material).

From the intraventricular high fidelity pressure signals we extracted the peak LV pressure, end-diastolic LV pressure, and the maximum of the first time derivative of LV pressure (dP/dt_{max}).

Echocardiographic Image Acquisition and Analysis

To avoid biological variability, all signals and images for measuring invasive and noninvasive indices of global systolic function were obtained simultaneously during the catheterization procedure. Broadband 2.0–4.0 MHz transducers were used either on a Vivid-7 or a Vivid-9 (General Electric Healthcare) system. Echocardiographic acquisitions were performed 5 minutes after completing the set of caval occlusions to define the ESPVR. Invasive tracings and images were synchronized by cross correlation of a signal connected to the ultrasound scanner and the hemodynamic signal acquisition system.[20, 21] LV volumes and ejection fraction were calculated using biplane Simpson method.[22] Mid-wall fractional shortening (MWFS) was calculated based on 2-dimensional measurements. Global longitudinal and circumferential strain (S) and strain rate (SR) were measured using commercial speckle-tracking software (EchoPac v. 110.1.2, General Electric) from the four chamber view and short chamber views, respectively (Figure 1, Panel B).

Color Doppler M-mode images were obtained and processed from the 5-chamber view and processed to obtain noninvasive indices derived from the intraventricular pressure difference waveform (see Supplemental Material).[23] Using custom-software, Doppler velocities are first decoded from the raw-velocity coded data stored in the DICOM images, via conversion to hierarchical data format.[24] Then, raw velocities are de-aliased, filtered and differentiated using smoothing splines. The 1-dimensional Euler's momentum equation is solved to obtain the M-mode distributions of the intraventricular pressure gradients along a center ejection

flow streamline (Figure 1, Panel C).[23] Finally, the pressure gradient distributions are integrated to obtain the pressure difference waveform between the LV apex and the outflow tract (Figure 1, Panel C).[9] EIVPD measurements have been previously validated in vivo[9] and clinical reproducibility in our laboratory has been reported.[20, 21]

Noninvasive estimations of maximal elastance were obtained using two previously reported single-beat methods that do not require preload manipulation.[10, 11] Method 1 ($E_{max\text{-}sb1}$), requires an empirical estimation of normalized "population-averaged" elastance at the onset of ejection (E_{Nd_avg}).[10] This normalized value is fitted by a seven-degree polynomial to the ratio of the pre-ejection to the total systolic ejection periods measured from Doppler spectrograms.[10] From this averaged value, normalized elastance at ejection onset (E_{Nd_est}) is then calculated from diastolic and end-systolic pressures (P_d and P_{es}, respectively)as:

$$E_{Nd\_est}=0.0275-0.165\cdot EF+0.3656(P_d/P_{es})+0.515\cdot E_{Nd\_avg}$$

and $E_{max\text{-}sb1}$ is obtained from systolic blood pressure P_s as:

$$E_{\max-sb1}=\frac{P_d-(E_{Nd\_est}\cdot P_s\cdot 0.9)}{SV\cdot E_{Nd\_est}}$$

For method 2, single-beat elastance is measured assuming a volume intercept of 0 mm Hg as:[11]

$$E_{\max-sb2}=\frac{P_{es}}{ESV}\approx\frac{P_s\cdot 0.9}{ESV}$$

To separate the error related to the inaccuracy of the non-invasive measurements from the error of the single beat methods themself, $E_{max\text{-}sb1}$ and $E_{max\text{-}sb2}$ were also calculated using conductance-derived volumes and invasive measurements of P_d and P_{es}.

To measure LV mass from LV real-time full-volume three-dimensional (3D) acquisitions, a second echocardiographic examination was performed in the echocardiography laboratory in the same day of the invasive procedure. All ultrasound measurements other than LV mass were obtained in the catheterization laboratory.

Statistical Analysis

Differences between hemodynamic data between patient groups (chest pain, dilated cardiomyopathy and patients with cirrhosis) were assessed by ANOVA following by Dunnet contrasts against the chest pain group. The correlation between noninvasive indices of systolic function and E_{max} was analyzed using the Pearson correlation coefficient (R), and corrected to avoid overfitting by bootstrap validation of 1000 repetitions (R_{boot}). Different regression slopes between E_{max} and noninvasive indices of systolic function was assessed by ANCOVA analysis.

Because neither preload nor afterload can be unequivocally characterized by a single hemodynamic measurement,[25] we integrated physiologically related variables into unique synthetic surrogates of load using data reduction strategies.[26] This approach of variable clustering simplifies regression modeling because it avoids trying to separate the effects of factors that are measuring the same phenomenon.[26] Thus, we calculated a synthetic index of preload as the first principal component of the principal components analysis (*R* software

version 3.0.1) based on the correlation matrix of LV end-diastolic pressure and LV end-diastolic volume. The correlation of the synthetic index with these two raw variables was R= 0.82 for both. We obtained the synthetic index of afterload integrating σ, Ea, and SVR using the same method. Correlation of these raw variables with the integrated afterload synthetic index was R= 0.90, 0.97, and 0.95, respectively. The effects of load confounders were analyzed using multiple linear regression models in which the noninvasive index was entered as the dependent variable, E_{max} as the independent variable, and LV mass, preload, and afterload as covariables. Standardized β coefficients were used to compare the effects of individual predictors. Regression diagnostics (outlier exclusion, normality of residuals with constant variance, and lack of significant interactions and nonlinearities) were performed for all these regression models. We used principal component analysis with illustrative variables to visualize the autocorrelation amongst noninvasive indices and their relationship with E_{max}, LV mass and load. Values of $P < .05$ were considered significant.

Results

Load and hemodynamic data

Cirrhotic patients typically showed low afterload, with low values of SVR, E_a, and σ (Table 2). Patients with dilated cardiomyopathy showed higher E_a, and σ, and a trend towards higher SVR. There was no significant difference among groups in LV end-diastolic pressure. E_{max} was reduced in patients with dilated cardiomyopathy, but not in patients with cirrhosis. All noninvasive indices except $E_{max\text{-}sb1}$ demonstrated impaired systolic chamber function in patients with dilated cardiomyopathy (Table 2). Mean differences of most indices were not significantly different between the liver cirrhosis and the chest pain groups.

Correlation between noninvasive indices and E_{MAX}

Peak-EIVPD showed the closest correlation with E_{max} (Table 3, Figure 2). Ejection fraction, MWFS and circumferential S and SR showed a significant but weaker correlation with E_{max}. $E_{max\text{-}sb2}$ showed a weak correlation with E_{max}, whereas $E_{max\text{-}sb1}$ failed to correlate with E_{max}. Even using volumes derived from the conductance catheter and invasive pressures in the single beat formula, $E_{max\text{-}sb1}$ did not correlate with E_{max} (R=0.04). Slopes of the EIVPD - E_{max} relationship were not different among patient groups (p=0.37).

Impact of load and mass onindices of systolic function

The multiple regression analysis of the hemodynamic determinants of the noninvasive indices is showed in Table 4. Peak-EIVPD and global circumferential S and SR were associated to systolic function (E_{max}) and were not significantly associated to LV mass, preload, or afterload. The magnitude of the association with E_{max} was highest for peak-EIVPD. Other indices such EF and MWFS were significantly associated to E_{max} but also to load variables. $E_{max\text{-}sb2}$ was only associated to LV mass, and $E_{max\text{-}sb1}$ and global longitudinal S and SR were influenced mostly by afterload(Table 4). Principal components analysis demonstrated that peak-EIVPD was the variable most closely associated to E_{max}, and that EF, longitudinal S, SR and $E_{max\text{-}sb1}$ were associated to afterload (Figure 3).

Discussion

This is the first clinical study to investigate the accuracy of ultrasound indices of systolic global chamber function by direct comparison with the invasive gold-standard method derived from the pressure-volume relationship. Using a between-subjects design in a group of patients with heterogeneous inotropic states and loading conditions, Doppler-derived peak-EIVPD showed the closest relationship with E_{max}. Other noninvasive indices such as EF, MWFS, and circumferential strain and strain rate showed a significant but weaker

correlation with the reference method. Longitudinal strain and strain rate were closer to afterload than to systolic function in this population.

Effects of load and systolic function on strain and strain-rate

The load dependence of strain and strain rate has been demonstrated in animal models,[27] but the inotropic sensitivity and relative effect of load on circumferential versus longitudinal strain are not well known in humans, and contradictory data has been published. A study in patients with normal or mildly impaired EF undergoing cardiac catheterization and acute loading interventions suggested that longitudinal strain is less sensitive to afterload than circumferential strain.[28] However, other studies indirectly suggest that circumferential strain may be more stable in patients with chronic abnormal afterload and secondary LV hypertrophy. In patients with aortic stenosis,[29] and hypertension[30] circumferential strain is preserved o even increased,[29] whereas longitudinal and radial strains are decreased. Moreover, in patients with aortic stenosis the afterload relief caused by aortic valve replacement results in an acute increase of longitudinal strain.[29] The absence of changes on circumferential in comparison to longitudinal strain measurements has been frequently interpreted as a lower inotropic sensitivity of circumferential function. The results of our study suggest that this may be more probably related to a lower load-dependency. Importantly, our study does not question the independent prognostic value of global longitudinal strain recently demonstrated in several conditions.[31, 32] As occurs with EF, the ability of longitudinal strain measurements to predict outcomes may be related to their capacity to amalgamatea number of variables related to integral pump performance.

EIVPD as an index of systolic chamber function

The inotropic sensitivity of the peak-EIVPD is based on established fluid dynamic principles,[33] and has been empirically confirmed in animals,[34] as well as in patients undergoing pharmacological interventions.[21] The potential use of Doppler-derived EIVPD as an index of LV systolic chamber function was first demonstrated in an animal experimental study that showed a close correlation with reference indices based on the pressure-volume relationship.[9] The present study confirms that peak-EIVPD closely correlates with E_{max} in patients, and supports its value as an index of LV systolic chamber function in the clinical setting. The relative load-independence of peak-EIVPD was also previously suggested by animal experimental data,[9] and is confirmed in the present clinical study. EVIPD reaches its peak very early during ejection, and this fact can probably explain its lower afterload dependence than other ejection phase indices. We believe that the closest relation with E_{max} and its relative load stability renders peak-EIVPD as one of the most robust and sensitive indices of LV systolic function available using echocardiography.

Noninvasive single-beat surrogates of maximal elastance

Combining LV volumes derived from echocardiography with peripheral arterial pressure has been proposed by several investigators as a surrogate method to noninvasively approximate the ESPVR.[10, 35] Our study demonstrates that these methods have important limitations related not only to the accuracy of the pressure and volume estimation, but also to the single-beat approach. The simplest method based on the ratio of end-systolic pressure and end-systolic volume ($E_{max\text{-}sb2}$) was closer related to E_{max} than the more complex method based on the estimation of the E_{Nd} ($E_{max\text{-}sb1}$). This result confirms that the estimation of E_{Nd} is the main source of inaccuracy in single-beat calculations, as previously demonstrated in experimental studies.[36] Some authors have assumed that E_{Nd} is a constant value in humans in the presence or absence of cardiac disease.[35] However, in ischemic cardiomyopathy it has been demonstrated that E_{Nd} differs quantitatively from normal hearts in all phases of the heart cycle.[37] In addition, for noninvasive application, E_{Nd} is estimated using a regression model derived from a small group of patients and based on noninvasive measurements of EF

and arterial load.[10] Our results suggest that application of this regression model to heterogeneous groups of patients can be misleading.

Limitations

The study was designed to comprehensively validate noninvasive methods against reference standards of global baseline systolic chamber function. Due to the relatively small patient group, validation results may deserve confirmation in a larger sample. We did not perform repeated measurements within subjects in order to avoid further complexity in the PV-loop catheterization procedure. Although a repeated measures design would have been useful for clarifying load dependence this design has been previously reported by our group in the animal setting.[9] Our aim was to analyze the value of different noninvasive indices to account for LV systolic chamber function. The evaluation of myocardial contractility is a different issue, very difficult to evaluate *in vivo*. It has been recognized that LV global systolic chamber function - and consequently E_{max}-, depends on myocardial contractility, muscle mass, and geometry. Only when mass and geometry are fixed, a shift of the ESPVR can be interpreted as a change in myocardial contractility. However, when evaluating patients with differences in LV mass and shape, as occurs in the clinical practice and in the present study, ESPVR reflects changes of chamber properties but not necessary of myocardial properties. Some authors have suggested normalizing E_{max} for muscle mass and geometry.[38] However, important limitations have been recognized for E_{max} normalization methods, particularly when relative wall thickness is abnormal.[39] We believe the results of our multiple regression and principal component analyses, showing an irrelevant role of LV mass as a confounder, suggests that mass normalization would not have modified the major findings of our study.

The method to obtain EVIPD is based on offline processing of digital color M-mode Doppler images using a custom-build algorithm that currently is not commercially available. This could limit the clinical application of this tool. However, computational requirements are very low and it could be easily incorporated into the analysis software of future ultrasound scanners to be used at bedside. Currently, strain and strain-rate measurements are increasingly used in clinical practice and also require offline processing.

All noninvasive indices tested in the present study have been obtained using Doppler-echocardiography. Other modalities such as magnetic resonance imaging provide a more accurate estimation of LV volumes, and tagging methods may also provide myocardial strain and strain rate measurements. However, our specific load sensitivity results suggest that limitations of indices of systolic chamber function are modality independent.

Clinical Implications

Relevant conclusions regarding the physiopathological mechanisms involved in heart failure have been supported on noninvasive single-beat estimators of pressure-volume indices. Noninvasive single-beat estimations of E_{max} has been used in the general population to analyze the effect of aging and gender on LV performance,[5] and to compare patients with heart failure and normal ejection fraction with control subjects.[6] The weak or absent between-subject correlation demonstrated in the present study makes a critical review of these previous studies necessary, and encourages the implementation of new Doppler-derived methods in the design of future large-scale studies.

Although EF is currently the pivotal index of systolic function in the clinical setting, under extreme or changing loading conditions its applicability is limited,[13, 40] and the use of novel noninvasive indices that correlate with E_{max} could add valuable diagnostic information. Peak-EIVPD arises as a reliable index of systolic function that provides additional information not captured by other noninvasive indices. Examples of potentially relevant

scenarios are situations of abnormal load, such as valve regurgitation, congenital heart disease, liver cirrhosis, systemic arteriovenous fistulae, or end-stage renal disease.

Conclusions

Noninvasive indices based on Doppler echocardiography have limited accuracy to characterize global LV systolic chamber function in the clinical setting. The Doppler-derived peak-EIVDP best correlates with reference indices. This index should be preferred for assessing the state of global LV systolic chamber function, particularly in conditions associated to abnormal load.

Supplementary Material

Refer to Web version on PubMed Central for supplementary material.

Acknowledgments

We are in debt with all the personnel of the Echocardiography and Catheterization Laboratories of the Hospital General Universitario Gregorio Marañón for their support for patient recruitment and data collection.

Sources of Funding

This study was supported by grants, PIS09/02603, RD12/0042 (RIC), RD06/0010 (RECAVA), CM12/00273 (to CPV) from the Instituto de Salud Carlos III, Ministerio de Economía y Competitividad, Spain. AGM and CPV were partially supported by grants from the Fundaciónpara la Investigación Biomédica Gregorio Marañón, Spain. PML is partially supported by NIH grant 1R21 HL108268-01.

Abbreviations

dP/dt_{max}	First time derivative of LV pressure with respect to time
E_a	Effective arterial elastance
EF	Ejection fraction
E_{max}	Maximal elastance
E_{max_sb1}	Single-beat E_{max} estimated by the normalized time-varying elastance method
E_{max_sb2}	Single-beat E_{max} estimated directly from systolic arterial pressure and end-systolic volume
E_{Nd}	Normalized time-varying elastance at arterial end-diastole
EIVPD	Ejection intraventricular pressure difference between the apex and the LV outflow tract
ESPVR	End-systolic pressure-volume relationship
MWFS	Mid-wall fractional shortening
P_{es}	End-systolic LV pressure
S	Strain
SR	Strain rate
SV	Stroke volume
SVR	Systemic vascular resistance
σ	End-systolic wall stress

References

1. Kosmala W, Jedrzejuk D, Derzhko R, Przewlocka-Kosmala M, Mysiak A, Bednarek-Tupikowska G. Left ventricular function impairment in patients with normal-weight obesity: contribution of abdominal fat deposition, profibrotic state, reduced insulin sensitivity, and proinflammatory activation. Circ Cardiovasc Imaging. 2012; 5:349–356.
2. Steendijk P, Meliga E, Valgimigli M, Ten Cate FJ, Serruys PW. Acute effects of alcohol septal ablation on systolic and diastolic left ventricular function in patients with hypertrophic obstructive cardiomyopathy. Heart. 2008; 94:1318–1322.
3. Yiu KH, Atsma DE, Delgado V, Ng AC, Witkowski TG, Ewe SH, Auger D, Holman ER, van Mil AM, Breuning MH, Tse HF, Bax JJ, Schalij MJ, Marsan NA. Myocardial structural alteration and systolic dysfunction in preclinical hypertrophic cardiomyopathy mutation carriers. PLoS One. 2012; 7:e36115. [PubMed: 22574137]
4. Sawaya H, Plana JC, Scherrer-Crosbie M. Newest echocardiographic techniques for the detection of cardiotoxicity and heart failure during chemotherapy. Heart Fail Clin. 2011; 7:313–321. [PubMed: 21749883]
5. Redfield MM, Jacobsen SJ, Borlaug BA, Rodeheffer RJ, Kass DA. Age- and gender-related ventricular-vascular stiffening: a community-based study. Circulation. 2005; 112:2254–2262.
6. Lam CS, Roger VL, Rodeheffer RJ, Bursi F, Borlaug BA, Ommen SR, Kass DA, Redfield MM. Cardiac structure and ventricular-vascular function in persons with heart failure and preserved ejection fraction from Olmsted County, Minnesota. Circulation. 2007; 115:1982–1990.
7. Rosen BD, Edvardsen T, Lai S, Castillo E, Pan L, Jerosch-Herold M, Sinha S, Kronmal R, Arnett D, Crouse JR 3rd, Heckbert SR, Bluemke DA, Lima JA. Left ventricular concentric remodeling is associated with decreased global and regional systolic function: the Multi-Ethnic Study of Atherosclerosis. Circulation. 2005; 112:984–991.
8. Greenberg NL, Firstenberg MS, Castro PL, Main M, Travaglini A, Odabashian JA, Drinko JK, Rodriguez LL, Thomas JD, Garcia MJ. Doppler-derived myocardial systolic strain rate is a strong index of left ventricular contractility. Circulation. 2002; 105:99–105. [PubMed: 11772883]
9. Yotti R, Bermejo J, Desco MM, Antoranz JC, Rojo-Alvarez JL, Cortina C, Allue C, Rodriguez-Abella H, Moreno M, Garcia-Fernandez MA. Doppler-derived ejection intraventricular pressure gradients provide a reliable assessment of left ventricular systolic chamber function. Circulation. 2005; 112:1771–1779.
10. Chen CH, Fetics B, Nevo E, Rochitte CE, Chiou KR, Ding PA, Kawaguchi M, Kass DA. Noninvasive single-beat determination of left ventricular end-systolic elastance in humans. J Am Coll Cardiol. 2001; 38:2028–2034.
11. Maurer MS, Sackner-Bernstein JD, El-Khoury Rumbarger L, Yushak M, King DL, Burkhoff D. Mechanisms underlying improvements in ejection fraction with carvedilol in heart failure. Circ Heart Fail. 2009; 2:189–196. [PubMed: 19808339]
12. Sagawa K, Suga H, Shoukas AA, Bakalar KM. End-systolic pressure/volume ratio: a new index of ventricular contractility. Am J Cardiol. 1977; 40:748–753.
13. Kass DA, Maughan WL, Guo ZM, Kono A, Sunagawa K, Sagawa K. Comparative influence of load versus inotropic states on indexes of ventricular contractility: experimental and theoretical analysis based on pressure-volume relationships. Circulation. 1987; 76:1422–1436. [PubMed: 3454658]
14. Bland JM, Altman DG. Statistics Notes: Correlation, regression, and repeated data. BMJ. 1994; 308:896.
15. Schrier RW, Arroyo V, Bernardi M, Epstein M, Henriksen JH, Rodes J. Peripheral arterial vasodilation hypothesis: a proposal for the initiation of renal sodium and water retention in cirrhosis. Hepatology. 1988; 8:1151–1157.
16. Kass DA, Midei M, Graves W, Brinker JA, Maughan WL. Use of a conductance (volume) catheter and transient inferior vena caval occlusion for rapid determination of pressure-volume relationships in man. Cathet Cardiovasc Diagn. 1988; 15:192–202.
17. Sunagawa K, Maughan WL, Burkhoff D, Sagawa K. Left ventricular interaction with arterial load studied in isolated canine ventricle. Am J Physiol. 1983; 245:H773–H780.

18. Arts T, Bovendeerd PH, Prinzen FW, Reneman RS. Relation between left ventricular cavity pressure and volume and systolic fiber stress and strain in the wall. Biophys J. 1991; 59:93–102.
19. Gaemperli O, Biaggi P, Gugelmann R, Osranek M, Schreuder JJ, Buhler I, Surder D, Luscher TF, Felix C, Bettex D, Grunenfelder J, Corti R. Real-time left ventricular pressure-volume loops during percutaneous mitral valve repair with the MitraClip system. Circulation. 2013; 127:1018–1027.
20. Yotti R, Bermejo J, Benito Y, Antoranz JC, Desco MM, Rodriguez-Perez D, Cortina C, Mombiela T, Barrio A, Elizaga J, Fernandez-Aviles F. Noninvasive estimation of the rate of relaxation by the analysis of intraventricular pressure gradients. Circ Cardiovasc Imaging. 2011; 4:94–104.
21. Yotti R, Bermejo J, Antoranz JC, Rojo-Alvarez JL, Allue C, Silva J, Desco MM, Moreno M, Garcia-Fernandez MA. Noninvasive assessment of ejection intraventricular pressure gradients. J Am Coll Cardiol. 2004; 43:1654–1662.
22. Lang RM, Bierig M, Devereux RB, Flachskampf FA, Foster E, Pellikka PA, Picard MH, Roman MJ, Seward J, Shanewise JS, Solomon SD, Spencer KT, Sutton MS, Stewart WJ. Recommendations for chamber quantification: a report from the American Society of Echocardiography's Guidelines and Standards Committee and the Chamber Quantification Writing Group, developed in conjunction with the European Association of Echocardiography, a branch of the European Society of Cardiology. J Am Soc Echocardiogr. 2005; 18:1440–1463. [PubMed: 16376782]
23. Bermejo J, Antoranz JC, Yotti R, Moreno M, Garcia-Fernandez MA. Spatio-temporal mapping of intracardiac pressure gradients. A solution to Euler's equation from digital postprocessing of color Doppler M-mode echocardiograms. Ultrasound Med Biol. 2001; 27:621–630.
24. Garcia D, Del Alamo JC, Tanne D, Yotti R, Cortina C, Bertrand E, Antoranz JC, Perez-David E, Rieu R, Fernandez-Aviles F, Bermejo J. Two-dimensional intraventricular flow mapping by digital processing conventional color-Doppler echocardiography images. IEEE Trans Med Imaging. 2010; 29:1701–1713.
25. Sagawa, K.; Maughan, WL.; Suga, H.; Sunagawa, K. Cardiac contraction and the pressure-volume relationship. New York: Oxford University Press; 1988. Physiological determinants of the ventricular pressure-volume relationship; p. 110-170.
26. Harrell, FE. Regression Modeling Strategies: With Applications to Linear Models, Logistic Regression, and Survival Analysis. In: strategies Mm. , editor. Regression Modeling Strategies: With Applications to Linear Models, Logistic Regression, and Survival Analysis. Springer; 2001. p. 53-84.
27. Weidemann F, Jamal F, Sutherland GR, Claus P, Kowalski M, Hatle L, De Scheerder I, Bijnens B, Rademakers FE. Myocardial function defined by strain rate and strain during alterations in inotropic states and heart rate. Am J Physiol Heart Circ Physiol. 2002; 283:H792–H799.
28. Burns AT, La Gerche A, D'Hooge J, MacIsaac AI, Prior DL. Left ventricular strain and strain rate: characterization of the effect of load in human subjects. Eur J Echocardiogr. 2010; 11:283–289.
29. Carasso S, Cohen O, Mutlak D, Adler Z, Lessick J, Reisner SA, Rakowski H, Bolotin G, Agmon Y. Differential effects of afterload on left ventricular long- and short-axis function: insights from a clinical model of patients with aortic valve stenosis undergoing aortic valve replacement. Am Heart J. 2009; 158:540–545.
30. Galderisi M, Esposito R, Schiano-Lomoriello V, Santoro A, Ippolito R, Schiattarella P, Strazzullo P, de Simone G. Correlates of global area strain in native hypertensive patients: a three-dimensional speckle-tracking echocardiography study. Eur Heart J Cardiovasc Imaging. 2012; 13:730–738.
31. Motoki H, Borowski AG, Shrestha K, Troughton RW, Tang WH, Thomas JD, Klein AL. Incremental prognostic value of assessing left ventricular myocardial mechanics in patients with chronic systolic heart failure. J Am Coll Cardiol. 2012; 60:2074–2081.
32. Buss SJ, Emami M, Mereles D, Korosoglou G, Kristen AV, Voss A, Schellberg D, Zugck C, Galuschky C, Giannitsis E, Hegenbart U, Ho AD, Katus HA, Schonland SO, Hardt SE. Longitudinal left ventricular function for prediction of survival in systemic light-chain amyloidosis: incremental value compared with clinical and biochemical markers. J Am Coll Cardiol. 2012; 60:1067–1076.

33. Pasipoularides A. Clinical assessment of ventricular ejection dynamics with and without outflow obstruction. J Am Coll Cardiol. 1990; 15:859–882.
34. Falsetti HL, Verani MS, Chen CJ, Cramer JA. Regional pressure differences in the left ventricle. Cathet Cardiovasc Diagn. 1980; 6:123–134.
35. Shishido T, Hayashi K, Shigemi K, Sato T, Sugimachi M, Sunagawa K. Single-beat estimation of end-systolic elastance using bilinearly approximated time-varying elastance curve. Circulation. 2000; 102:1983–1989.
36. Kjorstad KE, Korvald C, Myrmel T. Pressure-volume-based single-beat estimations cannot predict left ventricular contractility in vivo. Am J Physiol Heart Circ Physiol. 2002; 282:H1739–H1750.
37. Jegger D, Mallik AS, Nasratullah M, Jeanrenaud X, da Silva R, Tevaearai H, von Segesser LK, Stergiopulos N. The effect of a myocardial infarction on the normalized time-varying elastance curve. J Appl Physiol. 2007; 102:1123–1129.
38. Beyar R, Sideman S. Relating left ventricular dimension to maximum elastance by fiber mechanics. Am J Physiol. 1986; 251:R627–R635.
39. Burkhoff D, Mirsky I, Suga H. Assessment of systolic and diastolic ventricular properties via pressure-volume analysis: a guide for clinical, translational, and basic researchers. Am J Physiol Heart Circ Physiol. 2005; 289:H501–H512.
40. Quinones MA, Gaasch WH, Alexander JK. Influence of acute changes in preload, afterload, contractile state and heart rate on ejection and isovolumic indices of myocardial contractility in man. Circulation. 1976; 53:293–302.

Clinical Summary

An accurate and reliable assessment of left ventricular systolic remains a clinical challenge. Due to the well-known limitations of ejection fraction, a number of alternative methods have been implemented based on myocardial deformation, intraventricular flow dynamics, and single-beat estimations of the end-systolic pressure-volume relationship. In research and clinical practice, these noninvasive methods are increasingly used to assess systolic function in a number of disease conditions. The purpose of our study was to validate these new methods against maximal elastance obtained from invasive pressure and volume recordings. Specifically, we selected a population with a wide range of loading conditions including patients with chest pain and normal ejection fraction, dilated cardiomyopathy and liver cirrhosis. Our results showed that the Doppler-derived peak ejection intraventricular pressure difference was the index that most closely correlated with the reference method. Longitudinal strain-based deformation indices and noninvasive surrogates of maximal elastance were heavily influenced by afterload. In this study, the peak ejection intraventricular pressure difference was the most reliable index to characterize global systolic chamber function in the individual patient. Our findings show that this index is a reliable surrogate of maximal elastance in the clinical setting and may be particularly useful to assess intrinsic LV systolic function. Prospective clinical studies are justified to clarify the definite role of Doppler-derived ejection intraventricular pressure difference for guiding patient care in these scenarios.

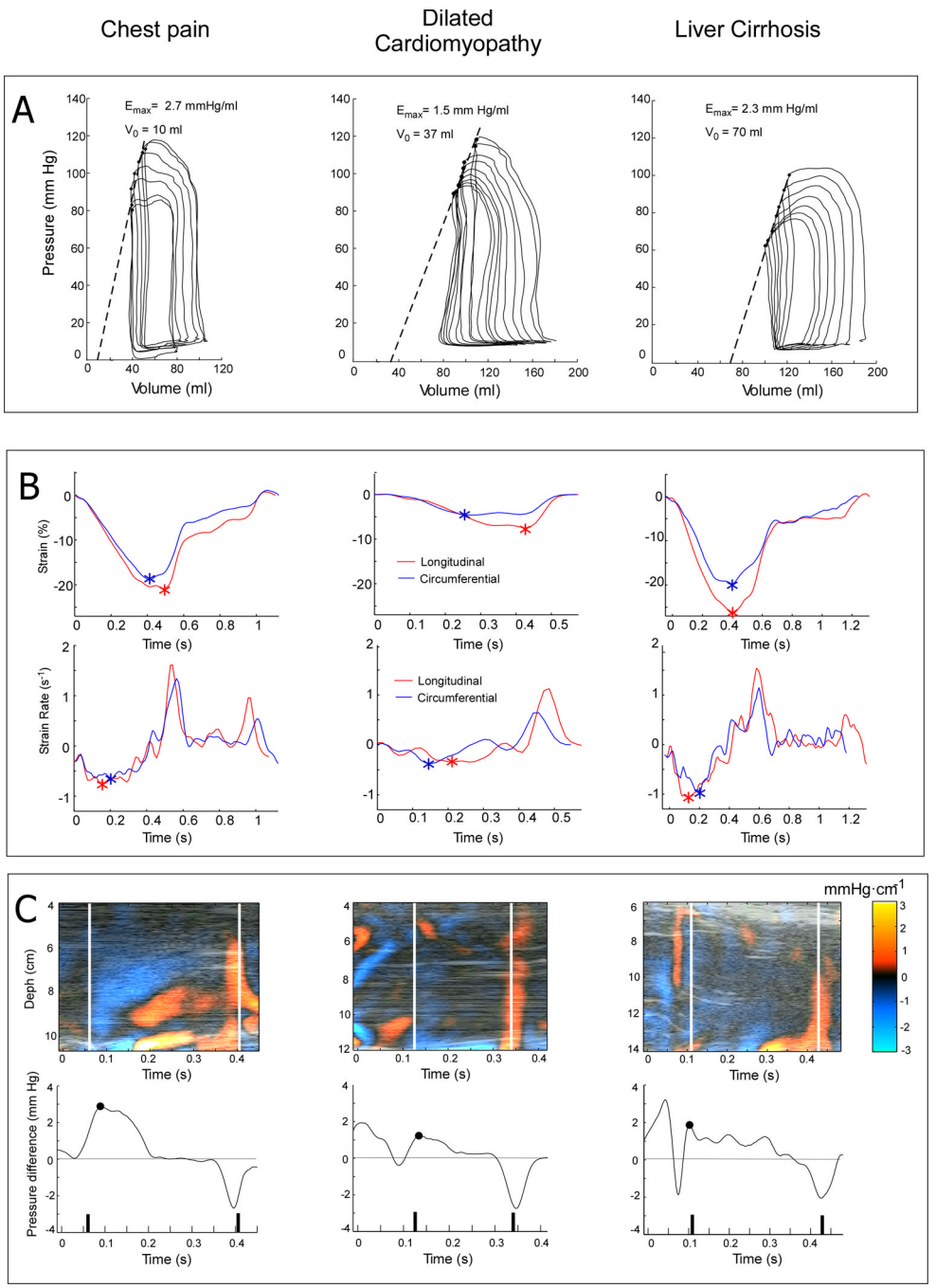

Figure 1.

Examples of invasive and echocardiographic indices of LV systolic function in representative patients with chest pain and normal EF (left), dilated cardiomyopathy (center) and liver cirrhosis (right). **Panel A**. Pressure-volume loops obtained during inferior vena cava occlusion. Maximal elastance (E_{max}) is obtained as the slope of the ESPVR. **Panel B**. Circumferential (blue) and longitudinal (red) global strain and strain rate tracings obtained from 2-dimensional echocardiographic images using speckle-tracking software; the peak global strain and strain rate are depicted (*). **Panel C**. Intraventricular pressure gradient maps obtained by post-processing color Doppler M-mode images (upper row) and pressure

difference waveforms between the apex and the outflow tract (lower row). The peak ejection intraventricular pressure difference (peak-EIVPD) is depicted in each curve (•).

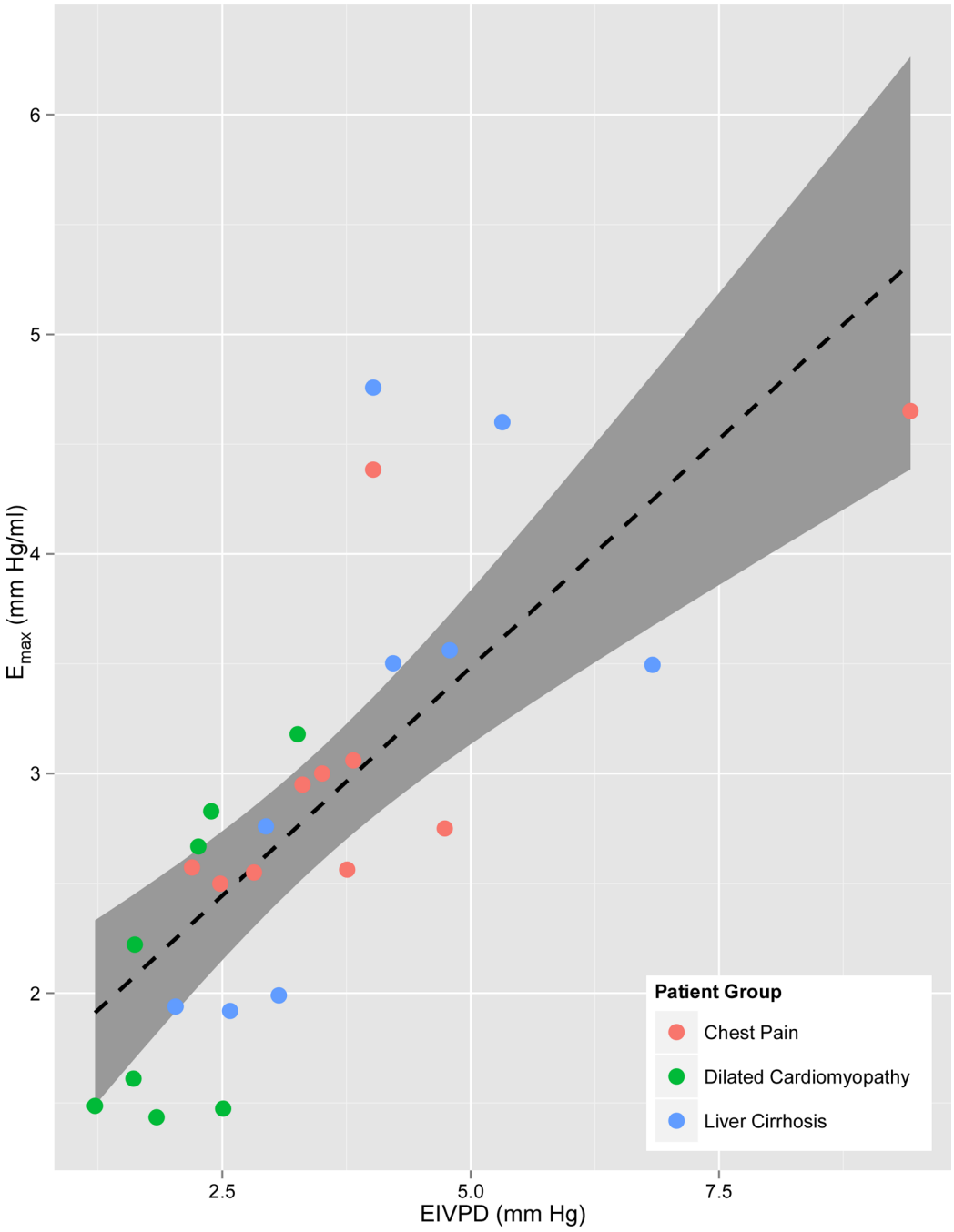

Figure 2.
Scatterplot, linear fitting (dotted line) and 95% confidence interval for the fitting (grey ribbon) of Doppler-derived ejection intraventricular pressure difference (Peak-EIVPD) versus left ventricular maximal elastance (E_{max}).

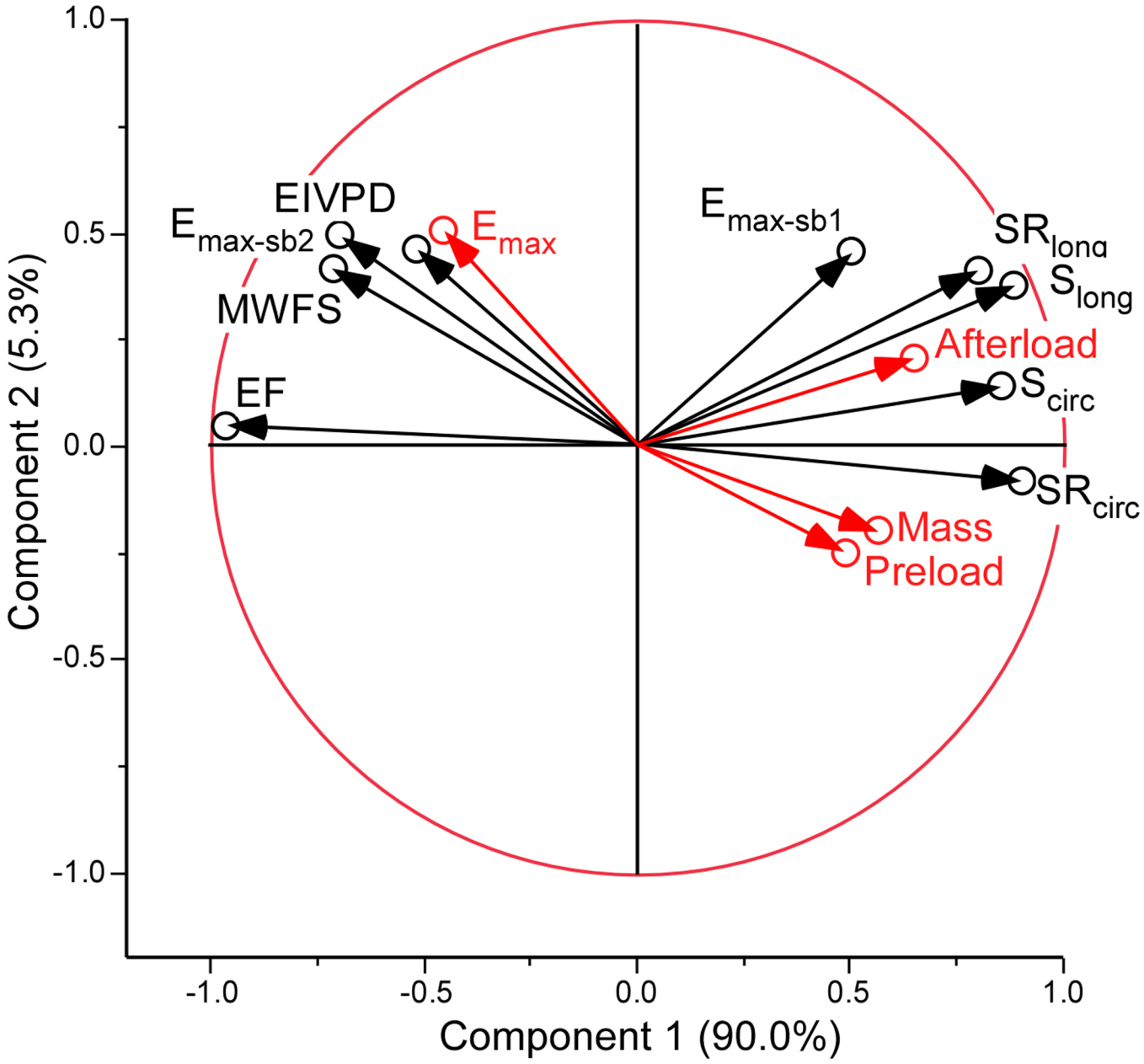

Figure 3.

Principal components analysis with illustrative variables. The autocorrelation of the noninvasive indices of systolic function (black circles) and their relationship with LV maximal elastance (E_{max}), mass, preload and afterload (red circles) is represented using a correlation circle. Axes represent the first (horizontal) and second (vertical) principal components (% of variation explained by each). The angle between two arrows represents the correlation between the respective variables. There is a positive correlation if the angle is small (variables are close to each other), there is no linear correlation if the angle is 90°, and there is an inverse correlation if the angle is > 90°. The closer a variable is to the boundary circle of correlations (arrow length closer to 1), the better it can be reconstructed from the first two components. EIVPD: Ejection intraventricular pressure difference; EF: ejection fraction; MWFS: mid-wall fractional shortening; S_{circ}: Circumferential strain; SR_{circ}:

Circumferential strain rate; S_{long}: Longitudinal strain; SR_{long}: Longitudinal strain rate; $E_{max\text{-}sb1}$: Single-beat E_{max} estimated by method 1; $E_{max\text{-}sb2}$: Single-beat E_{max} estimated by method 2 (see text for details).

Table 1

Clinical and demographic data

n	27
Gender (F)	12 (44%)
Age (years)	58±11
Significant Coronary Artery Disease	3 (11%)
QRS > 120 ms	5 (55%)
Mitral regurgitation (III-IV/IV)	1 (12%)
Cardiovascular Risk Factors	
Hypertension	13 (48%)
Diabetes Mellitus	10 (37%)
Hipercolesterolemia	6 (22%)
Smoking	4 (15%)
Obesity	7 (27%)
Cardiovascular Drugs	
Beta-blockers	20 (74%)
ACEI/ARBs	16 (59%)
Aldosterone receptor antagonist	11 (41%9
Diuretics	15 (57%)

Mean ± standard deviation; n (%). ACEI: angiotensin conversion enzyme inhibitors; ARB: angiotensin receptor blockers

Table 2

Hemodynamic and Echocardiographic Data

	Total	Chest Pain	DCM	Liver cirrhosis	ANOVA *p* value
n	27	10	8	9	-
Heart Rate (bpm)	72 ± 14	70 ± 10	83 ± 17	66 ± 12	-
Catheterization Data					
Mean Arterial Pressure (mm Hg)	98 ± 19	102 ± 11	110 ± 20	82 ± 13*	0.001
dP/dt_{max} (mm Hg s^{-1})	1283 ± 327	1529 ± 242	957 ± 231*	1216 ± 212*	<0.001
Cardiac Output (l/min)	6.9 ± 2.4	6.2 ± 1.5	5.5 ± 1.5	8.9 ± 2.7*	0.003
Cardiac Index (l/min/m^2)	4.0 ± 1.2	3.9 ± 0.8	3.2 ± 0.8	4.8 ± 1.4	0.04
Right Atrial Pressure (mm Hg)	10 ± 4	8 ± 4	8 ± 5	12 ± 2*	<0.001
Mean Pulmonary Pressure (mm Hg)	24 ± 6	23 ± 5	27 ± 9	21 ± 6	0.5
Pulmonary Capillary Wedge Pressure (mm Hg)	15 ± 5	13 ± 3	17 ± 6	16 ± 5	0.4
Pulmonary Vascular Resistance (dyn·cm·s^{-5})	120 ± 69	137 ± 49	159 ± 66	57 ± 48*	0.005
Systolic Chamber Function					
E_{max} (mm Hg/ml)	2.8 ± 1.0	3.1 ± 0.8	2.1 ± 0.7*	3.2 ± 1.1	0.04
Preload					
End-Diastolic LV Volume (ml)	114 ± 46	88 ± 24	162 ± 49*	102 ± 34	0.003
End-Diastolic LV Pressure (mm Hg)	20 ± 7	18 ± 4	21 ± 10	20 ± 7	0.9
Preload Index	0.0 ± 1.2	−0.6 ± 0.6	0.9 ± 1.4*	−1.3 ± 1.1	0.03
Afterload					
End-Systolic Wall Stress (mm Hg)	348 ± 117	347 ± 76	454 ± 120*	257 ± 68*	<0.001
Effective Arterial Elastance (mm Hg/ml)	1.5 ± 0.7	1.6 ± 0.3	2.2 ± 0.7*	0.9 ± 0.3*	<0.001
Systemic Vascular Resistance (dyn·cm·s^{-5})	1191 ± 589	1301 ± 400	1624 ± 659	683 ± 273*	0.001
Afterload Index	0.0 ± 1.7	0.2 ± 0.9	1.5 ± 1.7*	−1.5 ± 0.7*	<0.001
Chamber Remodeling					
End-Systolic Volume (ml)	51 ± 38	28 ± 13	99 ± 37*	35 ± 11	<0.001
LV Mass (g)	140 ± 52	109 ± 17	184 ± 74*	134 ± 21	0.005
Noninvasive Systolic Chamber Function					

	Total	Chest Pain	DCM	Liver cirrhosis	ANOVA *p* value
Ejection Fraction (%)	54 ± 20	65 ± 7	26 ± 9*	65 ± 8	<0.001
Mid-Wall Fractional Shortening (%)	13 ± 6	15 ± 3	6 ± 1*	16 ± 6	<0.001
Global Circumferential Strain (%)	−14 ± 7	−19 ± 4	−6 ± 2*	−18 ± 2	<0.001
Global Circumferential Strain Rate (s^{-1})	−0.8 ± 0.3	−1.0 ± 0.3	−0.4 ± 0.1*	−1.0 ± 0.1	<0.001
Global Longitudinal Strain (%)	−16 ± 7	−19 ± 4	−8 ± 2*	−22 ± 5	<0.001
Global Longitudinal Strain Rate (s^{-1})	−0.8 ± 0.4	−0.9 ± 0.2	−0.4 ± 0.1*	−1.1 ± 0.4	<0.001
Peak-EIVPD (mm Hg)	3.4 ± 1.7	4.0 ± 2.0	2.1 ± 0.6*	4.0 ± 1.5	0.02
$E_{max\text{-}sb1}$ (mm Hg/ml)	1.6 ± 0.7	1.7 ± 0.5	2.0 ± 0.6	1.0 ± 0.4	0.02
$E_{max\text{-}sb2}$ (mm Hg/ml)	3.6 ± 1.9	5.3 ± 1.4	1.6 ± 0.6*	3.5 ± 1.3*	0.003

* $p < 0.05$:

Dunnet comparison against the group of patients with chest pain and normal EF. Values show mean ± standard deviation. dP/dt: derivative of LV pressure with respect to time. Peak-EIVPD: peak ejection intraventricular pressure difference between the apex and the outflow tract; E_{max} maximal elastance. $E_{max\text{-}sb1}$ single-beat E_{max} estimated by method 1; $E_{max\text{-}sb2}$ Single-beat E_{max} estimated by method 2.

Table 3

Correlations between noninvasive indices of LV systolic chamber function and E_{max}

	E_{max}	
	R	**R_{boot}**
Ejection Fraction	0.41*	0.30
Mid-Wall Fractional Shortening	0.51*	0.40
Peak-EIVPD	0.75*	0.69
Global circumferential strain	−0.53*	−0.45
Global circumferential Strain Rate	−0.46*	−0.34
Global longitudinal strain	−0.35	−0.16
Global longitudinal Strain Rate	−0.37	−0.17
$E_{max\text{-}sb1}$	−0.05	0.30
$E_{max\text{-}sb2}$	0.38*	0.25

* $p < 0.05$.

R: Pearson correlation coefficient; R_{boot} Bootstrap validation after 1000 repetitions. Other abbreviations as in Table 2.

Table 4

Hemodynamic Determinants of Noninvasive Indices of LV Systolic Chamber Function

	E_{max}	LV Mass	Preload	Afterload	Adjusted R^2
Ejection Fraction (%)	0.41*	0.04	−0.65*	−0.21	0.75
Mid-Wall Fractional Shortening (%)	0.33*	0.18	−0.59*	−0.47*	0.77
Peak-EIVPD (mm Hg)	0.75*	0.00	−0.06	−0.22	0.62
Global Circumferential Strain (%)	−0.36*	0.21	−0.09	0.31	0.46
Global Circumferential Strain Rate (s^{-1})	−0.38*	−0.08	0.58	0.15	0.45
Global Longitudinal Strain (%)	−0.24	0.00	0.39	0.38*	0.46
Global longitudinal Strain Rate (s^{-1})	−0.28	−0.02	0.44	0.69*	0.54
$E_{max\text{-}sb1}$ (mm Hg/ml)	−0.01	−0.25	−0.27	0.63*	0.31
$E_{max\text{-}sb2}$ (mm Hg/ml)	0.29	−0.52*	−0.19	0.17	0.45

* $p < 0.05$.

Standardized β coefficients obtained by multiple linear regression analysis.

Abbreviations as in Table 2.